Regulatory phosphorylation site tunes Phosphoglucomutase 1 as a metabolic valve to control mobilization of glycogen stores.

Sofía Doello [1], Niels Neumann [1], Philipp Spät [2], Boris Maček [2] and Karl Forchhammer [1*]

[1]Interfaculty Institute of Microbiology and Infection Medicine, University of Tübingen, Auf der Morgenstelle 28, 72076 Tübingen, Germany

[2] Department of Quantitative Proteomics, University of Tübingen, Auf der Morgenstelle 15, 72076 Tübingen, Germany

*Corresponding author: karl.forchhammer@uni-tuebingen.de

Classification: Biological Sciences; Microbiology

Key words: glycogen metabolism, phosphoglucomutase, glucose-6-phosphate dehydrogenase, phosphorylation, metabolic channeling, carbon flux, oxidative pentose phosphate cycle protein, cyanobacteria

Abstract

Regulation of glycogen metabolism is of vital importance in organisms of all three kingdoms of life. Although the pathways involved in glycogen synthesis and degradation are well known, many regulatory aspects around the metabolism of this polysaccharide remain undeciphered. Here, we used the unicellular cyanobacterium *Synechocystis* as a model to investigate how glycogen metabolism is regulated in dormant nitrogen-starved cells, which entirely rely on glycogen catabolism to restore growth. We found that the activity of the enzymes involved in glycogen synthesis and degradation is tightly controlled at different levels via post-translational modifications. Phosphorylation of phosphoglucomutase 1 (Pgm1) on a peripheral residue (Ser63) regulates Pgm1 activity and controls the mobilization of the glycogen stores. Inhibition of Pgm1 activity via phosphorylation on Ser63 appears essential for survival of *Synechocystis* in the dormant state. Remarkably, this regulatory mechanism seems to be conserved from bacteria to humans. Moreover, phosphorylation of Pgm1 influences the formation of a metabolon, which includes Pgm1, oxidative pentose phosphate cycle protein (OpcA) and glucose-6-phosphate dehydrogenase (G6PDH). Analysis of the steady-state levels of the metabolic products of glycogen degradation together with protein-protein interaction studies revealed that the activity of G6PDH and the formation of this metabolon are under additional redox control, likely to ensure metabolic channeling of glucose-6-phosphate to the required pathways for each developmental stage.

Significance statement

In this study, we showed that post-translational modification of phosphoglucomutase 1 (Pgm1) via phosphorylation at a peripheral residue is a key, evolutionary-conserved regulatory mechanism that controls the utilization of the glycogen reserves. We identified Pgm1 as a central metabolic valve, associating with oxidative pentose phosphate cycle protein (OpcA) and glucose-6-phosphate dehydrogenase (G6PDH) into a metabolon. This interaction is regulated by the phosphorylation state of Pgm1 and the redox state of OpcA, and probably allows direction of the carbon flux into the required metabolic pathways.

Introduction

Glycogen is the major carbohydrate storage compound in a broad range of organisms, from bacteria to humans. This polysaccharide is composed of glucose molecules connected by α,1-4 linkages and branched via α,1-6 linkages, and it is generally considered a carbon sink with energy-storage function. In humans, glycogen is mainly accumulated in the liver and skeletal muscle, and it constitutes a rapid and accessible form of energy that can be supplied to tissues on demand.[1] In many bacteria, glycogen plays a crucial role in survival to an ever-changing environment. It is usually synthesized and accumulated inside the cells under growth-limiting conditions at excess of a carbon source, and degraded when the supply of energy or carbon is not enough to maintain growth or viability, thus allowing cell survival in transient starvation conditions.[2] In cyanobacteria, which generally sustain cell growth by performing oxygenic photosynthesis, glycogen is synthesized towards the end of the day, when photosynthetically fixed carbon is in excess and cells need to prepare to survive the night.[3] Glycogen accumulation also occurs as a response to nutrient limitation. In fact, the greatest amount of glycogen accumulation in non-diazotrophic cyanobacteria, which are unable to fix atmospheric N_2, occurs under nitrogen starvation conditions.[4]

Nitrogen deprivation activates a genetically determined survival program in non-diazotrophic cyanobacteria, which has been extensively studied in the unicellular cyanobacterial strains *Synechococcus elongatus* and *Synechocystis* sp. PCC 6803 (from now *Synechocystis*).[5] When *Synechocystis* encounters nitrogen depletion, the intracellular carbon/nitrogen balance is disturbed, and growth can no longer be supported. This metabolic situation leads to rapid accumulation of glycogen, which serves as a sink for the excess of carbon.[5] In order to survive these starvation conditions, cells undergo an adaptation process termed chlorosis that involves the degradation of the light-harvesting complexes to avoid an excess of energy and reduction equivalents that are no longer consumed by anabolic reactions. As a result of the metabolic and morphological changes induced by nitrogen starvation, cells enter a dormant state, which allows them to survive adverse conditions for a prolonged period of time.[6] Upon nitrogen availability, the glycogen stores accumulated in dormant cells play a key role in the restoration of vegetative growth.[7] When dormant cells have access to a nitrogen source, their metabolism switches towards a heterotrophic mode. They turn off residual photosynthesis, while the production of energy and metabolic intermediates now entirely relies on glycogen catabolism.[8] This extraordinary situation, in which carbohydrate degradation can be completely separated from photosynthetic processes even in the presence

of light, makes awakening *Synechocystis* cells an excellent model to study the regulation of glycogen catabolism.

Although the metabolic pathways involved in glycogen synthesis and degradation are well known, many regulatory aspects around the metabolism of this polysaccharide remain to be deciphered. In nitrogen-starved *Synechocystis* cells, glycogen degradation is known to start soon after addition of a nitrogen source, and the enzymes responsible for this process have been identified (**Figure 1**).[7] However, how glycogen catabolism is induced in dormant cells has not yet been elucidated. The enzymes involved in glycogen metabolism are conserved from bacteria to humans. The glycogen phosphorylase and debranching enzyme are responsible for the excision of glucose molecules from the glycogen granule, releasing glucose-1-phosphate (glucose-1P) and glucose, respectively. Glucose-1P is then converted to glucose-6-phosphate (glucose-6P) by the phosphoglucomutase (Pgm), an evolutionary conserved enzyme that also catalyzes the reverse reaction, while glucose is converted to glucose-6P by the glucokinase (Glk). Glucose-6P is then metabolized by the glucose-6-phosphate dehydrogenase (G6PDH) and enters either the Entner-Doudoroff (ED) or the oxidative pentose phosphate (OPP) pathway. Even though *Synechocystis* also possess the enzymes to catabolize glucose-6P via the Embden-Meyerhof-Parnas (EMP) pathway, this route has been shown not to be relevant for resuscitation from nitrogen starvation. Intriguingly, most of the main glycogen catabolic enzymes are up-regulated during nitrogen starvation, although glycogen degradation does not start until a nitrogen source is available. This suggests that the activity of these enzymes must be tightly regulated: They must remain inactive when cells are dormant and be activated upon nitrogen availability. An exception to the abundance pattern of most glycogen catabolic enzymes is Pgm1, whose expression is suppressed under nitrogen starvation and activated during resuscitation.[8,9] Although *Synechocystis* possesses two Pgm isoenzymes, Pgm1 (*sll0726*) has been shown to be responsible for almost 97 % of the Pgm activity.[10] Pgm1 was recently identified as a phosphoprotein with two localized serine phosphorylation sites: Ser 63 and Ser 68. Ser 168, which is predicted to be in the catalytic center, shows diminished phosphorylation during chlorosis. On the contrary, the phosphorylation of Ser 63 strongly increases during nitrogen starvation, representing one of the most strongly induced phosphorylation events.[9] These findings prompted us to investigate the possible involvement of Pgm1 in the regulation of glycogen metabolism in resuscitating cells, enabling us to unravel some of the key regulatory mechanisms in glycogen catabolism, which seem to be conserved from bacteria to humans.

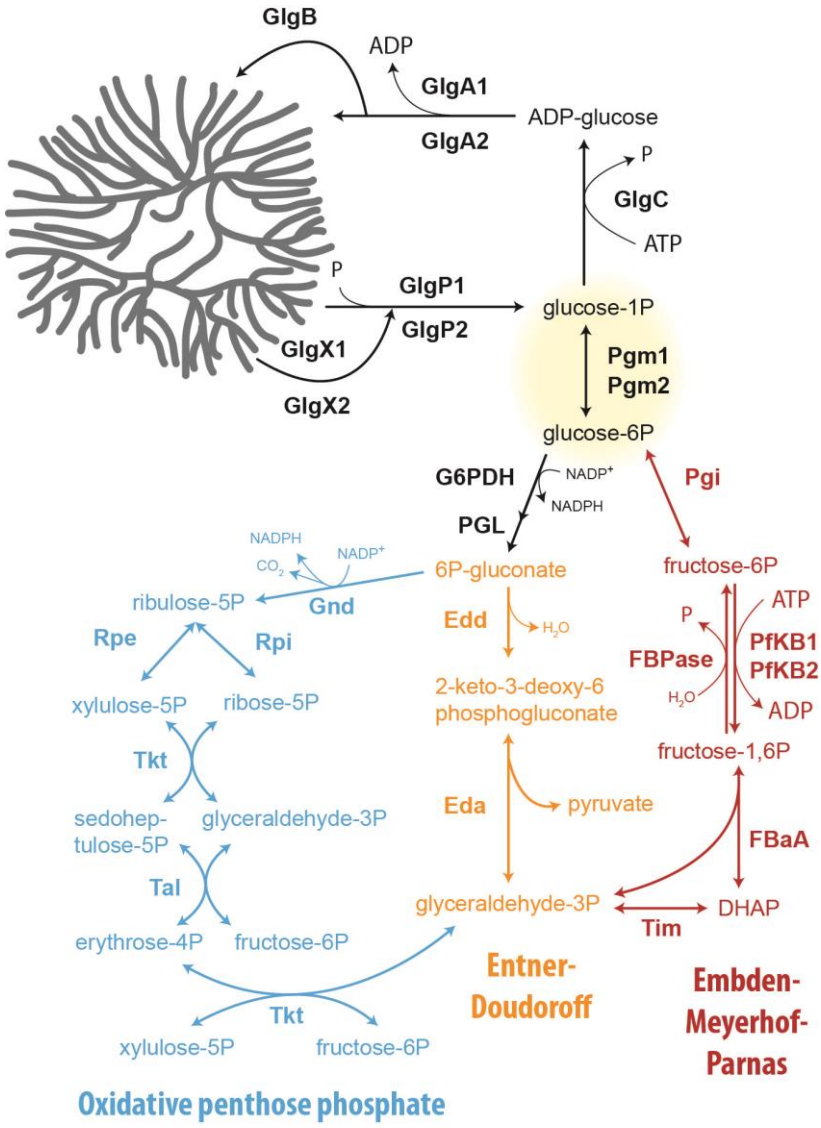

Figure 1. Schematic representation of the pathways involved in glycogen metabolism in *Synechocystis*.

Results

Pgm1 is activated during resuscitation from nitrogen starvation.

The transcription of the glycogen catabolic genes in *Synechocystis* is highly up-regulated during nitrogen deprivation,[11] when glycogen is synthesized, and turned down during resuscitation.[7] In a proteomic study covering the same developmental stages, Spät et al.[9] revealed that the glycogen catabolic enzymes are up-regulated in dormant and resuscitating cells (**Figure 2A**). One exception to this expression pattern is the Pgm1, the abundance of which is low during nitrogen starvation and increases during resuscitation (**Figure 2A**). In the same study, a quantitative analysis of the phosphorylation events during nitrogen starvation and resuscitation revealed that Pgm1 can be phosphorylated at two different residues: Ser 63

and Ser 168.[9] Interestingly, Ser 63 is one of the most phosphorylated residues in chlorotic cells, being 15 times more phosphorylated under nitrogen starvation than during vegetative growth (**Figure 2B**). These findings suggested that Pgm1 might be a regulatory point in glycogen catabolism. To test if there was any change in the activity of Pgm1 upon addition of a nitrogen source to dormant cells, we assayed Pgm1 activity in cell extracts from chlorotic and resuscitating cells (**Figure 2C**). While Pgm1 activity was detectable in cells under nitrogen starvation, the measured activity was 3 times higher in cells that had been supplemented with nitrate 24 hours before. These results suggested an activation of Pgm1 upon addition of nitrogen to chlorotic cells.

Given the high phosphorylation of the residue Ser 63 in nitrogen-starved cells, we speculated that Ser 63 might be a regulatory phosphorylation site. To determine whether phosphorylation of Pgm1 affects its activity, we treated cell extracts from chlorotic and resuscitating cells with alkaline phosphatase (AP) and measured Pgm1 activity before and after treatment. As shown in **Figure 2D**, a higher Pgm1 activity was measured after 10 min of treatment with AP in cells extracts from chlorotic, as well as from resuscitating cells. According to homology modeling of Pgm1, Ser 168 is the catalytic seryl-residue involved in the phosphor-exchange reaction and it is located in the active site of Pgm1 (**Figure 2E**). This catalytic serine is poorly phosphorylated during nitrogen starvation and it progressively becomes more phosphorylated during resuscitation (**Figure 2B**). Since phosphorylation of the catalytic serine is required for catalysis, the phosphorylation dynamics of this residue corresponds to its state of catalytic activity, with Pgm1 being inactive in chlorotic cells and becoming activated during resuscitation. Ser 63 follows the opposite pattern: The high level of phosphorylation of this residue under nitrogen starvation progressively decreases during resuscitation (**Figure 2B**). As deduced from homology modeling, Ser 63 is located on the surface of the enzyme, close to the access to the catalytic site (**Figure 2E**). Since Ser 168 is buried in the catalytic center, AP is more likely to dephosphorylate the surface-located Ser 63. Thus, the obtained results suggested that dephosphorylation of Ser 63 induces Pgm1 activity.

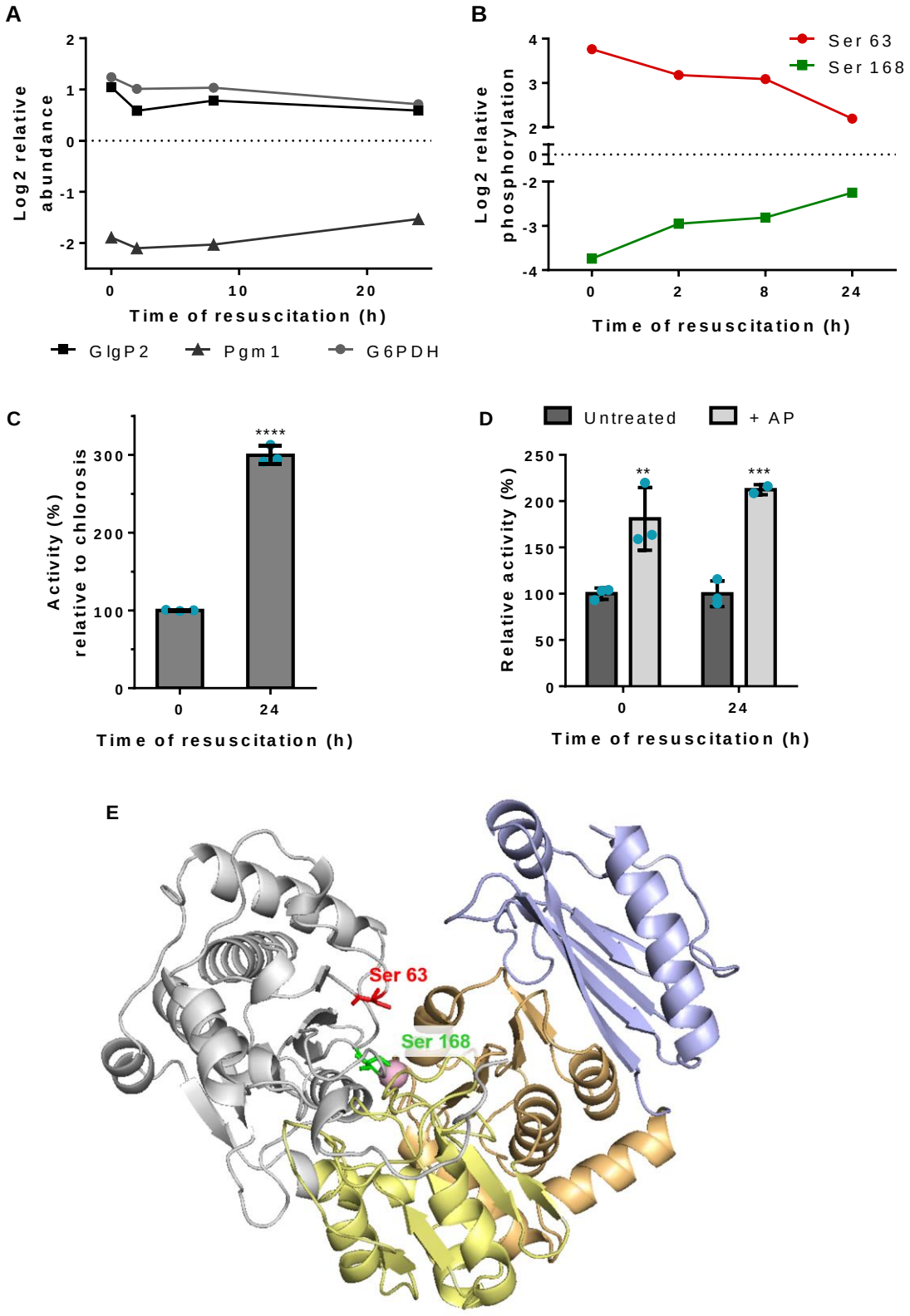

Figure 2. Abundance, phosphorylation and activity of Pgm1 during nitrogen starvation and resuscitation. (A) Protein abundance ratios of GlgP2, G6PDH and Pgm1 during resuscitation from nitrogen starvation. Ratios were calculated comparing the protein abundance during nitrogen starvation and resuscitation with their abundance during vegetative growth. Relative abundance is shown as the Log2 of the calculated ratios. Positive values indicate up-regulation and negative values down-regulation compared to protein levels during vegetative growth (normalized to zero, dotted line).[9] (B) Phosphorylation events of the two phosphorylation sites in Pgm1

at the indicated time points during resuscitation from nitrogen starvation. Ratios were calculated comparing the abundance of phosphorylated and unphosphorylated peptides at different time points during resuscitation to their abundance during vegetative growth. Relative phosphorylation is shown as the Log2 of the calculated ratios. [9] (C) Relative enzyme activity of Pgm1 in cell extracts from chlorotic and resuscitating cells. The activity in chlorotic cells was considered to be 100%. At least 3 biological replicates were measured. (D) Relative enzyme activity of Pgm1 in cell extracts from chlorotic and resuscitating cells before and after treatment with an alkaline phosphatase (AP) for 10 min. The activity before treatment was considered to be 100%. At least 3 biological replicates were measured. Error bars represent the SD, asterisks represent the statistical significance. (E) Structure of *Synechocystis'* Pgm1 obtained from Swiss Model using *Salmonella typhimurium's* Pgm as a template. The two colored resides shown in a stick model represent the two phosphorylation sites: Ser 63 in red and Ser 168 in green. The catalytic site is marked as a blue-shaded area and the Mg^{+} ion required for catalysis is shown as a pink sphere.

Pgm1 activity is regulated via phosphorylation at Ser 63.

To gain more insights on the effect of phosphorylation of Ser 63 in enzyme activity, we created different Pgm1 variants with site-specific amino acid substitutions and measured their activity *in vitro* (**Figure 3A**). First, Ser 63 was replaced by Asp (Pgm1 S63D) to create a phosphomimetic variant: in comparison to Ser, Asp is a larger, negatively charged amino acid that resembles a permanently phosphorylated Ser. The purified Pgm1 S63D seemed to be correctly folded, as deduced from its size exclusion chromatography elution profile (**Figure S1**). However, it presented very low activity *in vitro* (0.32 % of the WT activity), confirming that phosphorylation of Ser 63 inactivates Pgm1. In an attempt to create a Pgm1 variant that would mimic a permanently dephosphorylated enzyme, Ser 63 was substituted for Ala, Gly and Thr (Pgm1 S63A, S63G, and S63T, respectively). All of these variants showed a strongly reduced activity as compared to the wild-type (WT) Pgm1, with Pgm1 S63A presenting the highest activity of all variants (15 % of the WT Pgm1 activity). Comparison of the kinetic parameters of WT Pgm1 and Pgm1 S63A showed that the substitution of Ser for Ala at position 63 strongly affected the maximal velocity (V_{max}) of the reaction, which decreased almost 10-fold, but it did not decrease substrate affinity, as shown by the apparent Michaelis-Menten constant (K_m) (**Figure 3B**). In fact, the calculated K_m was even lower for Pgm1 S63A than for WT Pgm1. These results indicate that replacement of the residue S63 has a direct impact on the mechanism of catalysis rather than hindering substrate binding to the catalytic site.

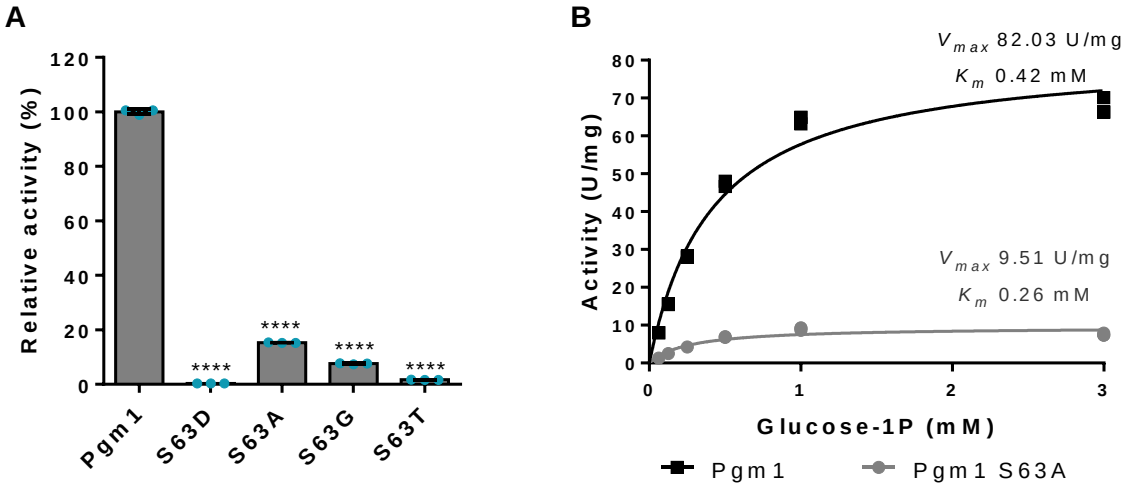

Figure 3. Phosphorylation of Ser 63 regulates Pgm1 activity. (A) Relative *in vitro* activity of wild type (WT) Pgm1 and different mutant variants. The activity of WT Pgm1 was considered to be 100%. At least 3 replicates were measured. Error bars represent the SD, asterisks represent the statistical significance. (B) Michaelis-Menten kinetics of WT Pgm1 (black squares) and Pgm1 S63A (grey circles). Three replicates were measured for each data-point.

Phosphorylation of Pgm1 at Ser 63 is essential for survival under nitrogen starvation.

So far, we could show that phosphorylation of Ser 63 regulates Pgm1 activity *in vitro*. In order to determine what role this regulatory phosphorylation plays during nitrogen starvation in *Synechocystis*, we created and characterized various Pgm1 mutant strains. A Pgm1 knockout strain (Δ*pgm1*) could not properly acclimate to nitrogen-depletion and presented a so-called non-bleaching phenotype: Cells did not degrade their photosynthetic pigments and turned yellow, but stayed greenish instead, progressively looking paler (**Figure 4A**). After two weeks of nitrogen starvation, a very reduced proportion of cells could recover when they were dropped on an agar plate containing nitrate, as compared to the WT (**Figure 4B**). Such a phenotype was previously observed in mutants that were impaired in glycogen synthesis,[12] since accumulation of this polymer has been shown to be indispensable for adaptation to nitrogen-starvation. This phenotype was expected, given that Pgm1 catalyzes the interconversion between glucose-1P and glucose-6P and is therefore involved in glycogen synthesis. Indeed, no glycogen was detected in seven-days-starved Δ*pgm1* cells (**Figure 4C**), indicating that Pgm1 activity is essential for glycogen synthesis under nitrogen deprivation, and that the activity of Pgm2 does not compensate the lack of Pgm1. Consequently, a strain with an inactive Pgm1 variant, such as the Pgm1 S63D, would not be able to enter the chlorotic state due to its inability to synthesize glycogen. To study the physiological consequences of the lack of Pgm1 inactivation via phosphorylation, we complemented the

Δ*pgm1* strain with the WT Pgm1 (Δ*pgm1*+Pgm1) and with the partially active Pgm1 S63A variant (Δ*pgm1*+Pgm1S63A), which lacks the phosphorylation site. Complementation with the WT protein rescued the phenotype: The Δ*pgm1*+Pgm1 strain showed a similar behavior than the WT under nitrogen starvation (**Figure S2A and B**). However, the Δ*pgm1*+Pgm1S63A strain was unable to acclimate to nitrogen deprivation (**Figure S2A and C**), indicating that the low activity of the Pgm1 S63A variant was not enough meet the cellular demand for Pgm activity. Therefore, we transformed wild-type cells with Pgm1 S63A (WT+Pgm1S63A) to study the impact of the lack of phosphorylation of residue 63 on long-term nitrogen starvation. As expected, this strain could initially acclimate to nitrogen depletion like the WT, since it contains the WT version of Pgm1. However, after prolonged exposure to these conditions, in which the WT version of Pgm1 would be highly phosphorylated, the cultures of the WT+Pgm1S63A strain progressively lost their characteristic yellowish color (**Figure 4A**). After one month of starvation, only a reduced number of cells could recover on a nitrate-containing agar plate (**Figure 4D**). WT+Pgm1S63A cells could synthesize glycogen upon nitrogen depletion, but after one week of starvation the glycogen content began to gradually decrease (**Figure 4E**). These findings imply that inactivation of Pgm1 via phosphorylation is crucial for preventing glycogen degradation during prolonged nitrogen starvation, which appears to be essential for survival of these conditions.

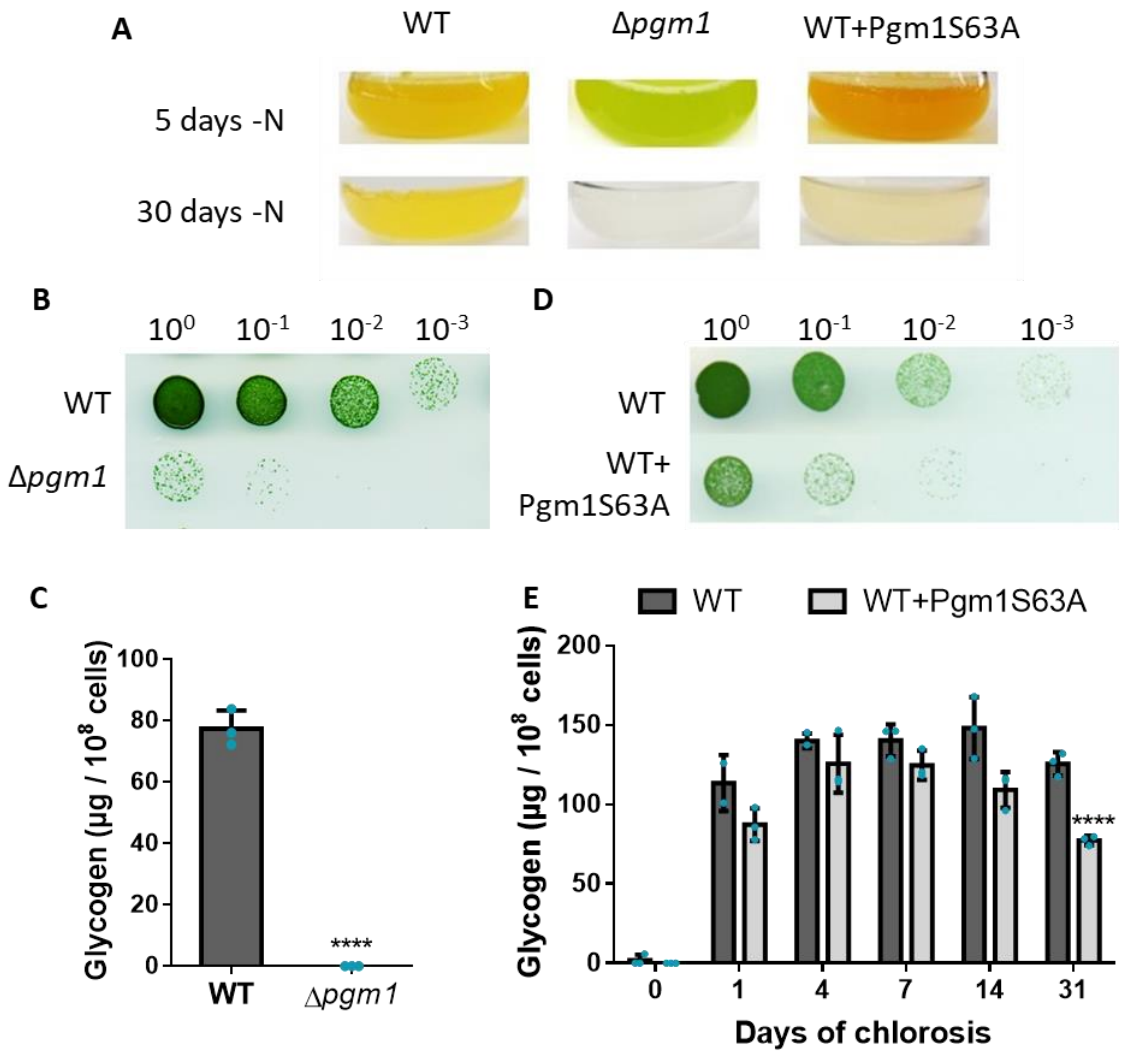

Figure 4. Pgm1 is required for glycogen synthesis and glycogen degradation during nitrogen starvation is prevented by phosphorylation of Ser 63. (A) Pictures of WT, Δ*pgm1*, and WT+Pgm1S63A cultures after 5 and 30 days of nitrogen starvation. (B) Recovery assay on a BG_{11}-agar plate of WT and Δ*pgm1*. Numbers on top represent the dilution factor, starting with an OD_{750} of 1. Pictures were taken 5 days after dropping chlorotic cells on the plate. (C) Glycogen content of WT and Δ*pgm1* after 7 days of nitrogen starvation. (D) Recovery assay of WT and WT+Pgm1S63A. (E) Glycogen content of WT and WT+Pgm1S63A at the indicated time points during nitrogen starvation. In all experiments, three biological replicates were measured. Error bars represent the SD; asterisks represent the statistical significance.

G6PDH activity is regulated by the redox state of its activator protein, OpcA.

To further prove the inactivation of Pgm1 under long-term nitrogen starvation in *Synechocystis*, the levels of glucose-phosphates in chlorotic and resuscitating cells were determined. Given the tight regulation of Pgm1, high levels of glucose-1P were expected in chlorotic cells, which should decrease upon nitrogen repletion. Indeed, an accumulation of glucose-1P during nitrogen starvation was detected: The levels of glucose-1P in chlorotic cells were approximately three times higher than in cells that were 21 h into resuscitation (**Figure 5**), confirming the inactivity of Pgm1 under nitrogen depletion. Intriguingly, glucose-

6P was also found to be accumulated in chlorotic cells (**Figure 5**). In fact, the levels of glucose-6P in both, chlorotic and resuscitating cells, were 100-fold higher than the levels of glucose-1P. This entails that the enzyme that metabolizes glucose-6P must also remain inactive under nitrogen-starvation. During recovery from chlorosis, glucose-6P has been shown to be metabolized mainly via the ED and OPP pathways,[8] implying that the enzyme responsible for glucose-6P catabolism is G6PDH.

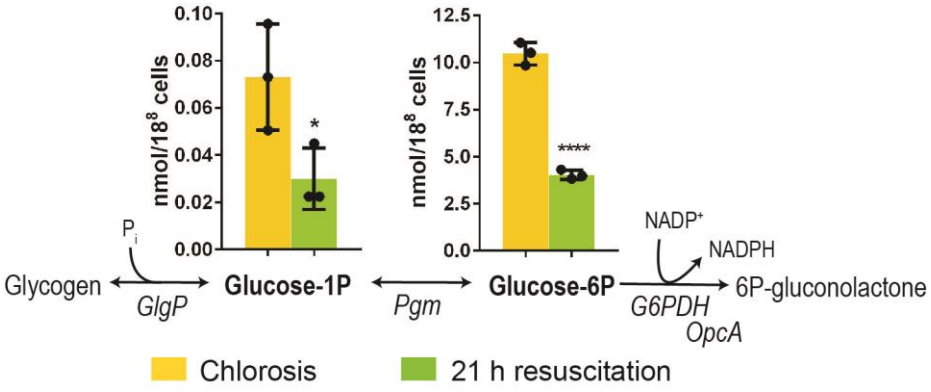

Figure 5. Glucose-phosphates accumulate in the cytoplasm during nitrogen starvation. Glucose-1P and glucose-6P content normalized to 10^8 cells during nitrogen starvation (yellow) and resuscitation (green). Three biological replicates were measured. Error bars represent the SD, asterisks represent the statistical significance.

We were then set to elucidate how G6PDH is regulated during nitrogen starvation in *Synechocystis*. In *Anabaena* sp. PCC 7120 and *Nostoc punctiforme*, the activity of G6PDH is known to be modulated by the redox state of the OPP cycle protein (OpcA), a protein that serves as an activator of G6PDH. OpcA is conserved in all cyanobacteria and it is required for G6PDH activity in *Anabaena* 7120, *N. punctiforme* and *Synechococcus* sp. 7942. In *Anabaena* 7120 and *N. punctiforme*, activation of G6PDH is modulated by the action of thioredoxin (Trx) on OpcA, which can only serve as an G6PDH activator in its oxidized state.[13,14] In the above-mentioned organisms, the *opcA* gene is located directly downstream from *zwf* (the gene encoding for G6PDH), while in *Synechocystis* these two genes are found in different operons. Moreover, the regulation of G6PDH might be different in *Synechocystis* than in nitrogen-fixing cyanobacteria, were this enzyme plays an important role in providing reduction power to the nitrogenase. Therefore, we purified G6PDH and OpcA from *Synechocystis* and studied the effect of the latter on G6PDH activity, as well as the effect of reducing and oxidizing agents on both proteins. As shown in **Figure 6A**, although G6PDH activity could be measured in the absence of OpcA, its substrate affinity increased by 6-fold when OpcA was added to the assay, confirming that OpcA acts as an allosteric activator of G6PDH in *Synechocystis*. When G6PDH was pre-incubated with reduced dithiothreitol

(DTT$_{red}$), trans-4,5-Dihydroxy-1,2-dithiane (DTT$_{ox}$) or $CuCl_2$ (which is known to induce formation of disulfide bonds), we could not detect any significant changes in G6PDH activity when the treated enzyme was assayed either in the absence or in the presence of untreated OpcA (**Figure 6B**), indicating that G6PDH itself is not sensitive to redox regulation. Pre-incubation of OpcA with DTT$_{red}$, on the other hand, reduced G6PDH activity to ~ 30 % as compared to the control, and this inhibitory effect could be partially reverted when the reduced OpcA was re-oxidized by treatment with DTT$_{ox}$. Moreover, pre-incubation of OpcA with *Synechocystis* thioredoxin TxrA had an even stronger inhibitory effect than DTT$_{red}$, reducing G6PDH activity to 10 %, which was the level of activity measured in the absence of OpcA. Pre-incubation of OpcA with DTT$_{ox}$ and $CuCl_2$ did not affect G6PDH activity, suggesting that the untreated OpcA was already in its oxidized state. These results show that in *Synechocystis*, like in the filamentous heterocyst-forming cyanobacteria, the activity of G6PDH is regulated by the redox state of OpcA.

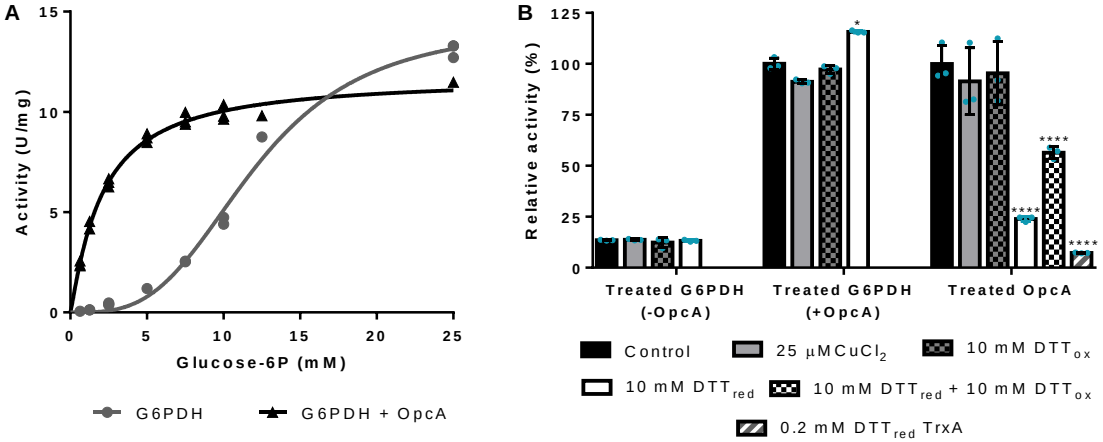

Figure 6. OpcA acts as an allosteric activator of G6PDH when it is in its oxidized state. (A) Effect of OpcA on the enzyme kinetics of G6PDH. OpcA was added as a 4:1 ratio to the amount of G6PDH. 3 replicates were measured for each data point. (B) Effect of incubating G6PDH or OpcA with reducing (DTT$_{red}$) and oxidizing (DTT$_{ox}$ and $CuCl_2$) agents on G6PDH activity. Assays were performed in the absence of the agents. 3 replicates were measured. Error bars represent the SD; asterisks represent the statistical significance.

Pgm1, OpcA and G6PDH form a complex to facilitate metabolic channeling.

The results presented above show the important role of Pgm1 phosphorylation in the regulation of glycogen metabolism. In an effort to find the protein phosphatase responsible for Pgm1 dephosphorylation during resuscitation, we analyzed the Pgm1 interactome through immunoprecipitation. Anti-Pgm1 antibodies were raised in rabbits and used to pull-down Pgm1 from cell extracts of resuscitating *Synechocystis* cells. Serum extracted from the

299 animals before immunization was used as a negative control. The proteins enriched in the
300 precipitate were analyzed by quantitative proteome analysis. No protein phosphatase was
301 found to be enriched, probably due to the transient interaction with their substrate.
302 Surprisingly, G6PDH and OpcA were significantly enriched in the precipitate (**Figure S3**).
303 Therefore, the interaction between these three proteins was analyzed in more detail using
304 biolayer interferometry (BLI). His8-tagged Pgm1 was immobilized on a Ni-NTA biosensor
305 and was allowed to associate with either Strep-tagged OpcA or Strep-tagged G6PDH. As a
306 negative control, His8-tagged PII-ΔT-loop (a truncated version of *Synechocystis* PII protein,
307 which is not expected to show interaction with the ligands) was immobilized to the biosensor
308 and Strep-tagged OpcA or Strep-tagged G6PDH were used as ligands (**Figure 7A**). OpcA
309 specifically bound to the sensor-immobilized Pgm1, but no binding of G6PDH to Pgm1 was
310 detected. We then studied the formation of the Pgm1-OpcA-G6PDH complex in a two-step
311 experiment, in which the sensor-immobilized Pgm1 was allowed to associate first to OpcA,
312 and then, in a second step, to G6PDH (**Figure 7B**). This experiment showed that G6PDH
313 could bind the sensor-bound Pgm1-OpcA complex, indicating that OpcA mediates the
314 formation of the Pgm1-OpcA-G6PDH complex.

315 Since the results above showed that OpcA can only induce G6PDH activity when it is in its
316 oxidized state, we studied the formation of the Pgm1-OpcA-G6PDH complex under reducing
317 and oxidizing conditions. The oxidized OpcA (treated with 5 mM DTT_{ox} for 30 min)
318 interacted with the immobilized Pgm1, while the reduced OpcA (treated with 5 mM DTT_{red}
319 for 30 min) showed very poor binding (**Figure 7C**). To analyze the interaction of reduced and
320 oxidized OpcA with G6PDH, His8-tagged G6PDH was immobilized to the Ni-NTA biosensor
321 and allowed to interact with either oxidized or reduced OpcA (**Figure 7D**). The oxidized
322 OpcA also showed better binding to the sensor-bound-G6PDH than the reduced OpcA. To
323 determine whether the redox state of Pgm1 and G6PDH also influences the formation of the
324 Pgm1-OpcA-G6PDH complex, the binding assays showed in **Figures 7C** and **7D** were
325 repeated after treating the immobilized proteins (Pgm1 and G6PDH, respectively) with
326 DTT_{red} or DTT_{ox}. The formation of the complex was slightly better when Pgm1 was in its
327 oxidized state (**Figure S4A**), whereas no difference was observed between the reduced and
328 oxidized G6PDH (**Figure S4B**). Interestingly, the phosphomimetic variant Pgm1 S63D did
329 not show any binding to OpcA (**Figure S4C**). These results indicate that, when Pgm1 is
330 dephosphorylated at Ser 63, it interacts with the OpcA-G6PDH complex in an oxidized state,
331 thus forming a dynamic supramolecular complex of sequential metabolic enzymes.

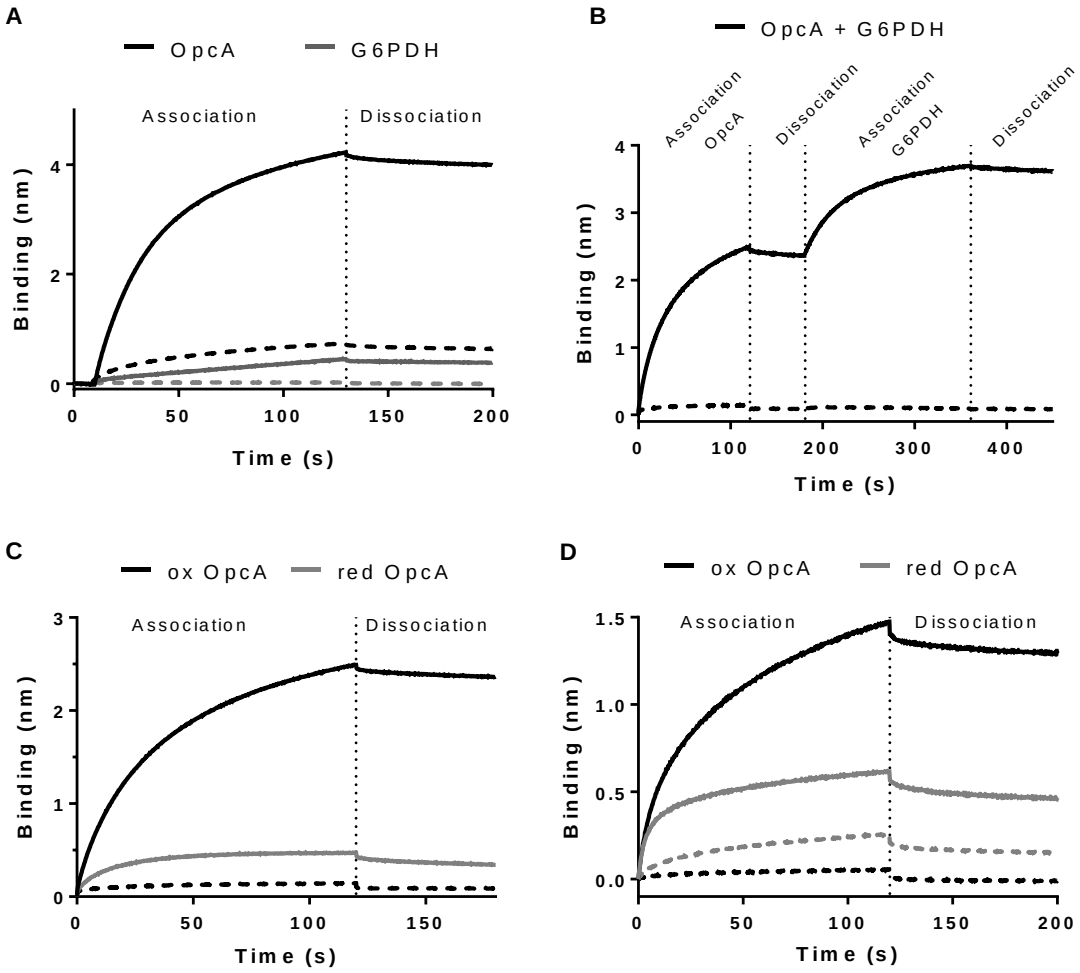

Figure 7. Pgm1, OpcA and G6PDH transiently form a metabolon under oxidized conditions. *In vitro* analysis by Biolayer Interferometry of the interaction between Pgm1, OpcA and G6PDH. Solid lines: (A)(B)(C) His8-tagged Pgm1 was immobilized on Ni-NTA sensor tips, (D) His8-tagged G6PDH was immobilized on Ni-NTA sensor tips. Dashed lines: His8-tagged PII-ΔT-loop was immobilized on Ni-NTA sensor tips. (A) Sensor-immobilized proteins were allowed to associate with either OpcA or G6PDH. (B) Sensor-immobilized proteins were allowed to associate first with OpcA, then with G6PDH. (C) Sensor-immobilized proteins were allowed to associate with oxidized or reduced OpcA. (D) Sensor-immobilized proteins were allowed to associate with oxidized or reduced OpcA.

To determine its size, the Pgm1-OpcA-G6PDH complex was further analyzed via multiangle light scattering coupled to size exclusion chromatography (SEC-MALS) (**Figure S5**). When G6PDH was analyzed alone, most of the protein eluted in a peak with a MALS-determined molar mass of 242.9 ± 0.02 kDa, which corresponds to the tetrameric state of G6PDH (4 x 59 kDa). Additionally, a smaller peak corresponding to the monomeric G6PDH was detected, with a determined molar mass of 59.56 ± 0.071 KDa (**Figure S5A**). OpcA and Pgm1 alone mostly eluted as monomers (55.26 ± 0.009 kDa and 63.61 ± 0.025 kDa, respectively), although higher oligomeric states were also detected (**Figure S5B and C**). When G6PDH was mixed with OpcA in equimolar concentrations, a dominant peak with a

molar mass of 430.3 ± 0.02 kDa was observed, in addition to small amounts of monomeric OpcA (**Figure S5D and F**). The mass difference between the tetrameric G6PDH (4 x 59 kDa) and the G6PDH-OpcA complex (430 kDa) agrees with 4 subunits of OpcA (55 kDa) binding to the tetrameric G6PDH. Analysis of G6PDH, OpcA and Pgm1 together in equimolar concentrations revealed a new peak with a molar mass of 705.57 ± 0.009 kDa, in addition to the previously detected peak of 430 kDa for the OpcA- G6PDH complex (**Figure S5E and D**). The apparent mass difference of 275 kDa agrees with four subunits of Pgm (4 x 63 kDa) binding to the OpcA-G6PDH complex. Overall, the tetrameric G6PDH seems to bind 4 monomers of OpcA, each of which binds a Pgm1 monomer, forming a complex that appears to be stable due to the lack of decay detected in the chromatograms.

Pgm1 regulation is conserved from bacteria to humans.

Regulation of Pgm activity is crucial for the survival of a wide range of organisms to many different conditions. Interestingly, a homologous residue of the phosphorylation site Ser 63 of *Synechocystis* Pgm1 is also found in higher mammals, such as humans, mice and rabbits (**Figure 8A**). In humans, Pgm1 deficiency leads to glycogenosis, a metabolic disorder that causes the abnormal use and storage of glycogen.[15] Despite the importance of the correct activity of this enzyme on human health, little is known regarding its functional regulation. Although Ser 20 of the human Pgm1 (HPgm1), which is the homologous residue of *Synechocystis* Pgm1 Ser 63 in the human protein, has been identified as a phosphorylation site,[16] the role of phosphorylation of this residue has not been investigated. To ascertain whether phosphorylation of HPgm1 at Ser 20 has a similar effect than phosphorylation of Ser 63 in *Synechocystis* Pgm1, we purified HPgm1 along with a mutant variant, in which Ser 20 had been substituted by Asp (HPgm1 S20D), and measured their enzyme activities *in vitro*. As shown in **Figure 8B**, HPgm1 S20D showed no enzyme activity, indicating that, as in *Synechocystis*, HPgm1 activity may be regulated by phosphorylation at Ser 20.

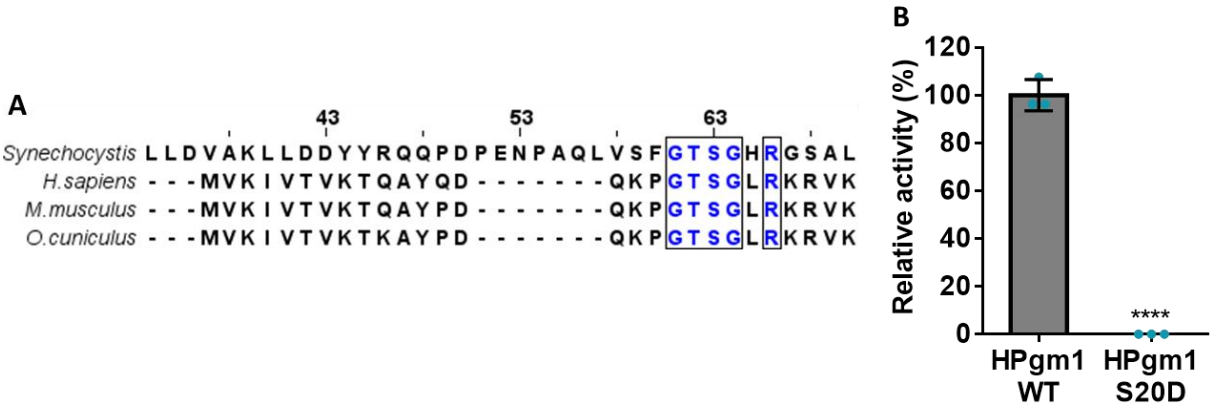

Figure 8. Regulation of Pgm1 by phosphorylation is conserved in mammals. (A) Alignment of the sequence of Pgm1 from *Synechocystis*, *Homo sapiens*, *Mus musculus* and *Oryctolagus cuniculus*. The conserved motif is marked in blue. (B) Relative *in vitro* activity of HPgm1 and HPgm1 S20D. The activity of WT Pgm1 was considered to be 100%. At least 3 replicates were measured. Error bars represent the SD; asterisks represent the statistical significance.

Discussion

Regulation of glycogen metabolism is of vital importance in organisms of all three kingdoms of life. In bacteria, proper control of glycogen synthesis and degradation determines the ability to survive transient periods of nutrient starvation. In mammals, deficiencies in glycogen metabolism lead to a variety of different metabolic disorders, some of them very severe. In this study, we used the unicellular cyanobacterium *Synechocystis* to investigate the regulatory mechanisms of some of the key glycogen metabolic enzymes.

During nitrogen starvation, the activity of the glycogen catabolic enzymes must be regulated to prevent premature glycogen degradation, so that cells can use this reserve polymer once the conditions are favorable for resuscitation. We could show that this control is exerted by the combined regulation of Pgm1 and G6PDH: Pgm1 is inactivated by phosphorylation of Ser 63, whereas G6PDH is under a tight redox control.

Pgm is an evolutionary conserved enzyme that mediates one of the most important reactions in carbohydrate metabolism: It catalyzes the interconversion between glucose-1P and glucose-6P, being thereby involved in both, glycogen synthesis and degradation.[17] Despite its important role in sugar metabolism, Pgm activity has only recently started to be considered as a target for metabolic control.[18–21] At the onset of nitrogen starvation, the activity of the Pgm1 isoform is required for glycogen synthesis, as shown by the inability of a Pgm1 knock-out mutant to synthesize glycogen. Once enough glycogen has been accumulated, Pgm1 activity is inhibited by phosphorylation of Ser 63. When in addition to the WT Pgm1, the non-phosphorylated S63A variant is present, cells degrade glycogen after

prolonged nitrogen starvation and concomitantly lose viability. This highlights the pivotal role of Ser 63 phosphorylation for controlling glycogen catabolism. This residue is highly phosphorylated in long-term-chlorotic cells and it is progressively de-phosphorylated during resuscitation. *In vitro* characterization of a phosphomimic variant of Pgm1 (Pgm1 S63D) strongly suggests that the phosphorylated version of the enzyme is inactive. Analysis of other Pgm1 variants (Pgm1 S63A, S63G, and S63T) indicated that substitution of Ser 63 affects catalysis, as their V_{max} was much lower as compared to WT Pgm1, although the substrate affinity was not impaired (as deduced from the K_m value). Based on structural studies of the reaction mechanism from related proteins,[22] we suggest a role of Ser 63 in a conformational change occurring during catalysis. When Pgm1 is in its open conformation, its catalytic cleft is easily accessible for phosphorylated sugars. When glucose-P enters the catalytic site, the unphosphorylated end of the sugar binds the phosphorylated Ser 168 (see **Figure 2**). The phosphorylated end of the glucose molecule must interact with the phosphate-binding residues present in domain 4. In order for these residues to come in close contact, Pgm1 must undergo a conformational change that involves a rotation of domain 4 and changes the active site from an open cleft to a closed pocket. This conformational change requires the interaction of a group of residues from domain 4 with a group of residues from domain 1, including Ser 63.[23] This explains why any change of Ser 63 has a negative effect on catalysis. When the site of Ser 63 is occupied by a negative residue, as in the phosphomimetic variant, or when the seryl-residue is phosphorylated, the negative charge obstructs this conformational change, preventing the closed conformation of the enzyme and thereby inhibiting catalysis.

Strikingly, this regulatory phosphorylation site located in domain 1 of Pgm1 is conserved in higher organisms, including mouse, rabbit and human. Although Pgm1 deficiency can cause severe disease in humans, its functional regulation remains under-investigated. HPgm1 is known to be phosphorylated and thereby activated by the p21-activated signaling kinase 1 (Pak1) on Thr 466.[17] However, although Ser 20, the homologous of *Synechocystis* Ser 63, had previously been reported as a phosphorylation site in HPgm1,[16] the role of this phosphorylation on enzyme activity had not been characterized. We were able to demonstrate that, as in *Synechocystis*, HPgm1 is also inactivated by phosphorylation at Ser 20. In agreement with our results, a study involving patients suffering from Pgm1 deficiency showed that mutations on the loop in domain 1 where Ser 20 is located in HPgm1 led to a reduced enzyme activity (3.3% of the control) and caused moderate disease in heterozygote patients. [23] These findings suggest that the regulatory mechanism discovered in this study is evolutionary conserved.

Analysis of the steady-state levels of metabolites of glycogen degradation showed high accumulation of glucose-6P, implying that Pgm1 is not the only control point, but also the enzymes that catalyze the glucose-6P consuming reactions are regulated. Although catabolism of the bulk of the glycogen reserves must be prevented during nitrogen starvation, residual glycogen synthesis and degradation constantly takes place in chlorotic cells:[24] A residual carbon flux through the glycogen catabolic pathways results in synthesis of polyhydroxy butyrate (PHB) during prolonged nitrogen starvation. The data presented here also supports the existence of such residual flux, given the considerable glycogen degradation and loss of viability in the WT+Pgm1S63A strain after long-term starvation. This minimal metabolic activity is necessary to maintain the minimum ATP levels to keep viability in dormant cells.[25] As mentioned above, glycogen can be catabolized via three different routes: The EMP, the ED and the OPP pathways. G6PDH directs glucose-6P into the OPP and ED pathways, whereas the glucose-6-phosphate isomerase (Pgi) leads it into the EMP pathway. Koch et al.[24] showed that the main carbon flux from glycogen to PHB synthesis in chlorotic cells happens through the EMP pathway, which is the route with the highest ATP yield, whereas the OPP and ED pathways seem to play a minor role in this process. Our data indicate that G6PDH is inactive in chlorotic cells. The cytoplasm of nitrogen-starved cells is a reducing environment: When cells are nitrogen-depleted, anabolic processes stop consuming the electrons provided by photosynthetic reactions and reducing equivalents accumulate.[26] Under these conditions, OpcA should be reduced by the Trx system, and would be unable to activate G6PDH. However, when a nitrogen source is added to chlorotic cells, the glycogen pool is mainly mobilized through the ED and OPP pathways, and not through the EMP pathway. Although the latter is energetically more productive than the OPP and ED pathways, it does not generate the necessary metabolic intermediates to re-built the previously degraded cellular components in nitrogen-starved cells and it is therefore not the preferred route for carbohydrate degradation during resuscitation[8], or during heterotrophic growth in general.[27] Upon addition of a nitrogen source, the glutamine synthetase – glutamate synthetase (GS-GOGAT) nitrogen assimilation cycle is immediately induced.[7,25] The GOGAT reaction, which produces glutamate from glutamine and 2-oxoglutarate, consumes reduction equivalents, thereby alleviating the over-reduced state of the cytoplasm, which would allow activation of G6PDH by OpcA and utilization of the ED and OPP pathways.

Oxidation of OpcA and dephosphorylation of Pgm1 triggered by nitrate addition also allows the formation of the Pgm1-OpcA-G6PDH complex. Although transient interaction between sequential metabolic enzymes has been observed in a variety of pathways, the

purpose of enzyme assembly remains uncertain. Control of the metabolic flux at a branch point of a pathway has been proposed as a key role of enzyme complex formation: Enzyme assembly may allow channeling of the metabolic product from one enzyme to the next one, avoiding its use by a competing enzyme at a branch point in a metabolic network. In such case, the enzymatic complexes are known as metabolons. However, the functional significance of metabolon formation has not yet been fully clarified.[28] Catabolism of glucose-6P represents a branch point in glycogen degradation. The data derived from the characterization of mutants in key enzymes of the glycogen catabolic pathways strongly suggests that, upon nitrogen addition, the carbon flow is switched from the EMP to the ED and OPP pathways,[8,24] although both G6PDH and Pgi are up-regulated in recovering cells,[9] suggesting the existence of a regulatory mechanism in the control of metabolic flux. We propose that the Pgm1-OpcA-G6PDH complex acts as a metabolon that channels glucose-6P towards the ED and OPP pathways, which provide the metabolites and reduction equivalents required for resuscitation from chlorosis, thereby preventing it from being utilized by Pgi. The fact that the interaction between OpcA, Pgm1 and G6PDH is favored under oxidizing conditions and when Pgm1 is dephosphorylated suggests that formation of the Pgm1-OpcA-G6PDH complex is induced during the transition to heterotrophic growth, when functionality of the OPP and ED pathways is required. Thus, the Pgm1-OpcA-G6PDH metabolon is probably also relevant in the light-dark transitions. Altogether, our study sheds new light on the regulation of the central glycogen metabolic hub, which is at the core of carbohydrate metabolism. Tight regulation of the bi-directional Pgm1 is thereby of special relevance, with its regulation through seryl-phosphorylation being evolutionary conserved from cyanobacteria to humans.

Acknowledgements

We thank Samuel Quinzer for his involvement in G6PDH enzymatic assays, Dr. Nicolas Nalpas for his help with the proteomics data, and Dr. Libera Lo Presti for her assistance writing this manuscript. This work was supported by the German Research Council (DFG) FOR 2816 “The Autotrophy-Heterotrophy Switch in Cyanobacteria: Coherent Decision-Making at Multiple Regulatory Layers”. LC-MS/MS systems at the Department of Quantitative Proteomics were supported by the DFG grants INST 37/935-1 and INST 37/741-1 FUGG. Additionally, we acknowledge the infrastructural support from EXC 2124 “Controlling Microbes to Fight Infections”.

Author contributions

S.D. performed cultivation experiments, cloning, protein purification, enzymatic assays, glycogen and glucose-phosphate determinations, BLI experiments, SEC-MALS experiments, constructed mutants, analyzed data, and wrote manuscript with input from all authors. N.N. contributed cloning and BLI experiments. P.S performed proteomic analysis. K.F. conceived study, interpreted data and edited manuscript.

Competing interests

The authors declare no competing financial interest.

Methods

Cyanobacterial cultivation

The cyanobacterial strains used in this study are listed in **Table S1**. All strains were grown in BG_{11} supplemented with 5 mM $NaHCO_3$ for vegetative growth, as described previously.[29] Nitrogen starvation was induced as previously described by a 2-step wash with BG_{11-0} medium supplemented with 5 mM $NaHCO_3$, which contains all BG_{11} components except for $NaNO_3$.[7,30] Resuscitation was induced by addition of 17 mM $NaNO_3$ to cells residing in BG_{11-0}. Cultivation was performed with continuous illumination (50 to 60 µmol photons m−2 s−1) and shaking (130 to 140 rpm) at 27 °C. Mutant strains were cultivated with the appropriate concentration of antibiotics.[8] All strains used for this study are shown in **Table S1**. Biological replicates were inoculated from the same pre-cultures, but propagated, nitrogen-starved and resuscitated independently in different flasks under identical conditions.

Protein overexpression and purification

Escherichia coli Rosetta-gami (DE3) was used for the overexpression of all proteins. All primers and plasmids used for protein overexpression are shown in **Table S2** and **Table S3**, respectively. Cells were cultivated in 2xYT (1L of culture in 5L flasks) at 37 °C until they reached exponential growth (OD_{600} 0.6-0.8) and protein overexpression was then induced by adding either 0.1 mM IPTG (for His-tagged proteins) or 75 µg/L anhydrotetracycline (for Strep-tagged proteins), followed by incubation at 20°C for 16 h. Cells were harvested by centrifugation at 4000 g for 10 min at 4 °C, and disrupted by sonication in 40 mL of lysis

buffer (100 mM Tris-HCl pH 7.5, 150 mm KCl, 5 mM $MgCl_2$, 10 mM imidazole (only for His-tagged proteins), DNAse, and protease inhibitor cocktail). The cell lysates were centrifuged at 20,000 g for 1 h at 4°C and the supernatants were filtered with a 0.22 µM filter.

For the purification of His-tagged proteins, 1 mL Ni-NTA HisTrap columns (GE Healthcare, Illinois, USA) were used. The cell extracts were loaded into the columns, washed with wash buffer (100 mM Tris-HCl pH 7.5, 150 mm KCl, and 50 mM Imidazole) and eluted with elution buffer (100 mM Tris-HCl pH 7.5, 150 mm KCl, and 500 mM Imidazole).

For the purification of Strep-tagged proteins, 5 mL Ni-NTA Strep-tactin® superflow (Qiagen, Maryland, USA) columns were used. The cell extracts were loaded into the columns, washed with wash buffer (100 mM Tris-HCl pH 7.5 and 150 mm KCl) and eluted with elution buffer (100 mM Tris-HCl pH 7.5, 150 mm KCl, and2.5 mM desthiobiotin).

The buffer of all purified proteins was exchanged via dialysis using dialysis buffer (100 mM Tris-HCl pH 7.5, 150 mm KCl, and 5 mM $MgCl_2$) and a 3 kDa cutoff dialysis tube. 1 mm DTT was also added to the dialysis buffer for Pgm1 and HPgm1. All purifications were checked via SDS-PAGE.

Measurement of Pgm activity in cell extracts

To determine the Pgm activity in *Synechocystis* cell extracts an assay was adapted from Osanai et al.[31] The Pgm reaction was coupled to the G6PDH reaction and the glucose 6-phosphate-dependent conversion of $NADP^+$ to NADPH was monitored by measuring the absorbance at 340 nm. Cells were harvested by centrifugation at 4000 g for 10 min at 4 °C, resuspended in lysis buffer (100 mM Tris-HCl pH 7.5, 10 mM $MgCl_2$) and disrupted by using a "FastPrep®-24"(MP Biomedicals). The lysate was centrifuged for 10 min at 4 °C before the protein content was determined. When indicated, cell lysates were treated with 2 U/mL of alkaline phosphatase for 1 h at 37 °C. Approximately 50 µg of protein were used for each reaction. The reaction buffer was composed of 100 mM Tris-HCl pH 7.5, 10 mM $MgCl_2$, 1 mM $NADP^+$, 1 mM DTT and 1 U/mL G6PDH from *Saccharomyces cerevisiae* (G6378, Sigma Aldrich, Missouri, USA). The reaction was started by the addition of 10 mM glucose-1P. Absorption change at 340 nm was continuously measured for 15 min at 30 °C. As a blank, the change in absorption in the absence of glucose-1P was also measured and subtracted from the experimental values. The enzymatic activity was then calculated. At least three biological replicates were measured.

561 **Measurement of Pgm activity *in vitro***

562 The reaction buffer was composed of 100 mM Tris-HCl pH 7.5, 150 mM KCl, 10 mM
563 $MgCl_2$, 1 mM $NADP^+$, 1 mM DTT and 1 U/mL G6PDH from *Saccharomyces cerevisiae*
564 (G6378, Sigma Aldrich). 100 ng of His-tagged purified Pgm were added to each reaction. The
565 reaction was started by the addition of glucose-1P and 40 µM glucose-1,6-bisphosphate.
566 Absorption change at 340 nm was continuously measured for 15 min at 30 °C. The enzymatic
567 activity was then calculated. At least three replicates were measured.

568 **Measurement of G6PDH activity *in vitro***

569 The reaction buffer was composed of 100 mM Tris-HCl pH 7.5, 150 mM KCl, 10 mM
570 $MgCl_2$ and 1 mM $NADP^+$. 500 ng of Strep-tagged purified G6PDH were added to each
571 reaction. When indicated, OpcA was added on 1:4 molar ratio to G6PDH. When stated, the
572 enzymes were pre-treated with DTT_{red}, DTT_{ox} or $CuCl_2$ at the concentration and for the time
573 indicated in the figure legends, but enzyme activity was always measured in the absence of
574 reducing or oxidizing agents. The reaction was started by the addition of 10 mM glucose-6P.
575 Absorption change at 340 nm was continuously measured for 15 min at 30 °C. The enzymatic
576 activity was then calculated. At least three replicates were measured.

577 **Recovery assay**

578 Serial dilutions of chlorotic cultures were prepared (10^0, 10^{-1}, 10^{-2}, 10^{-3}, 10^{-4} and 10^{-5})
579 starting with an OD_{750} of 1. 5 µl of these dilutions were dropped on solid BG_{11} agar plates and
580 cultivated at 50 µmol photons m^{-2} s^{-1} and 27 °C for five days.

581 **Glycogen determination**

582 Glycogen content was determined as described by Gründel et al.[12] with modifications
583 established by Klotz et al.[7] 2 mL-samples were collected, span down and washed with
584 distilled water. Cells were lysed by incubation in 30% KOH at 95°C for 2h. Glycogen was
585 precipitated by addition of cold ethanol to a final concentration of 70% followed by an
586 overnight incubation at -20 °C. The precipitated glycogen was pelleted by centrifugation at
587 15000 g for 10 min and washed with 70% ethanol and 98% absolute ethanol, consecutively.
588 The precipitated glycogen was dried and digested with 35 U of amyloglucosidase (10115,
589 Sigma Aldrich) in 1 mL of 100 sodium acetate pH 4.5 for 2 h. 200 µl of the samples were
590 mixed with 1 mL of 6% O-toluidine in acetic acid and incubated at 100 °C for 10 min.

Absorbance was then read at 635 nm. A glucose calibration curve was used to determine the amount of glycogen in the samples. For every condition, at least three biological replicates were measured.

Glucose-phosphate quantification

4 mL of chlorotic and resuscitating (24 h after $NaNO_3$ addition) were harvested (OD_{750} ~ 0.8) by centrifugation at 18,000 g for 1 min at 4°C. Pellets were immediately frozen in liquid nitrogen. Cells were lysed by addition of 0.2 M HCl and incubation at 95 °C for 15 min. Lysates were centrifuged at 18,000 g for 10 min at room temperature, then the supernatants were transferred to clean 2 mL tubes. Samples were neutralized with 1 mL of 1 M Tris-HCl pH 8. A glucose-1P and glucose-6P calibration curve were prepared. $NADP^+$, KCl, and $MgCl_2$ were added to samples and standard solutions to a final concentration of 1 mM, 150 mM and 10 mM, respectively. The absorbance of samples and standards were measured at 340 nm (blank measurement). 3 U of G6PDH from *Saccharomyces cerevisiae* (G6378, Sigma Aldrich) were added to all samples and standards and their absorbance at 340 nm was measured after incubation for 5 min at room temperature (glucose-6P measurement). 3 U of Pgm from rabbit muscle (P3397, Sigma) were added to all samples and glucose-1P standards and their absorbance at 340 nm was measured after incubation for 5 min at room temperature (glucose-1P measurement). The blank measurements were subtracted from the glucose-6P measurements, and the glucose-6P standard curve was used to determine the concentration of glucose-6P in the samples. The glucose-6P measurements were subtracted from the glucose-1P measurements, and the glucose-1P standard curve was used to determine the concentration of glucose-1P in the samples. Data were normalized to the OD_{750} of the sampled cultures. Three biological replicates were measured.

Pull down assay

A pull down assay was performed 4 h after the addition of nitrate to chlorotic cells. Therefore, 250 mL cultures of *Synechocystis* cells were cultivated and nitrogen-starved as described above in three independent biological replicates per condition. Cells were harvested by centrifugation at 4,000 x g for 10 min and cell pellets were resuspended in 2 mL of lysis buffer (50 mM Tris-HCl, pH 7.4) before lysis with a FastPrep®-24 Ribolyser at 4 °C (3 cycles at 7.5 m s-1 for 30 s and 5 min breaks in between). Cell extracts were centrifuged at 16,000 x g for 5 min at 4 °C and supernatants were transferred to a new 1.5 mL tubes. Protein

G Magnetic Beads were aliquoted (150 µl) and washed twice with 1 mL of lysis buffer. Then either pre-immune serum or post-immunization anti-Pgm1 antiserum (PINEDA, Berlin, Germany) was added to the beads and they were incubated for 10 min at RT under agitation on an orbital shaker. Beads were washed again and incubated with the cell extracts for 10 min at RT, then washed again. Proteins were eluted in 2 consecutive steps with 60 µl of elution buffer (200 mM glycine, pH 2.5) each. Both fractions were combined and protein concentration was measured. Pull down eluates were precipitated by the addition of 9 sample volumes of a 8:1 v/v ice-cold acetone:methanol mixture and incubated o.n. at -20°C. Protein precipitates were pelleted (5 min 1000 x g at RT) and washed twice with each 1 mL 80% v/v acetone aq. The resulting protein pellet was air-dried and resuspended in 20 µL denaturation buffer. Protein concentrations were measured by Bradford assay and 10 µg protein per sample were treated with dithiothreitol (1 mM) and subsequently iodoacetmaide (5.5 mM) for each 60 min at RT. Samples were digested with 1 µg Lys-C for 3 h, then diluted 1:5 with 20 mM ABC buffer pH 8.0 followed by addition of 1 µg trypsin and incubation o.n. at RT while shaking. The peptide solution was cleaned by stage-tips.[32] LC-MS analysis was performed as described before on a Q Exactive HF or HF-X as described elsewhere.[9] Raw data was analyzed via MaxQuant 1.6.8.0 using a Target/Decoy Database from Cyanobase (*Synechocystis* sp. PCC 6803; 10.06.2014, user-modified) with 3671 protein IDs. Label -free quantification algorithm was used to calculate LFQ intensities. Data from all pull down experiments was analyzed via the Perseus software (version 1.6.5.0). For the identification of significantly enriched proteins, a t-test was performed with the following requirements: each protein had to be detected in at least two replicates and an FDR of 0.001 at S0 = 0.3 was set.

Biolayer interferometry using the Octet K2 system

Protein-protein interaction was tested *in vitro* by biolayer interferometry using the Octet K2 system (FortéBio). All experiments were performed in HEPES buffer (100 mM HEPES-KOH PH 7.5 and 10 mM $MgCl_2$). For the experiments with one Association/Dissociation step, either His8-Pgm1 or His8-tagged G6PDH was immobilized on Ni-NTA sensor tips (FortéBio) by exposing the sensors to a 500 nM solution of Pgm1 for 120 s (Loading), followed by a 60 s baseline measurement. To avoid unspecific binding, the sensor tips were then dipped in a solution containing 600 nM of His8-PII, followed by a second 60 s baseline measurement. For the binding of OpcA and Zwf, the sensor tips dipped in either a 500 nM solution of Strep-OpcA or a 500 mM solution of Strep-G6PDH for 120 s (Association). When indicated, these proteins were pre-treated with either 5mM DTT_{red} or 5 mM DTT_{ox} for 30

min. The assay was finalized with a 120 s Dissociation step. As a control, Loading was done using His8-PII instead of His8-Pgm1. For the experiments with two Association/Dissociation steps, the sensors tips were first loaded with Pgm1 as described above. In the first Association step, the sensors were exposed to a 500 nM Strep-OpcA solution, followed by a first Dissociation step. In the second Association step, the same sensors were dipped in a 500 nM Strep-G6PDH solution, followed by a second Dissociation step. As a control, Loading was done using His8-PII-ΔT-loop instead of His8-Pgm1. The biosensors were regenerated after each use with 10 mM glycine (pH 1.7) and 10 mM $NiCl_2$ as proposed in manufacturers recommendations. The recorded curves were aligned to the baseline before the Association step.

Size exclusion chromatography multiangle light scattering (SEC-MALS)

SEC-MALS experiments were performed using an ÄKTA purifier system connected to a Superose 6 Increase 10/300 GL column (GE healthcare) at a flow rate of 0.4 ml/min in running buffer (100 mM Tris-HCl pH 7.5, 150 mM KaCl, and 10 mM MgCl2). The column was calibrated using the gel filtration calibration kit LMW and HMW (GE Healthcare) according to the manufacturer's instructions. To analyze the oligomeric state of the recombinant proteins, the ÄKTA micro was connected to downstream MALS using the miniDAWN TREOS combined with an Optilab T-rEX refractometer (Wyatt Technology, Dernbach, Germany). Data analysis was performed using the software ASTRA 7 (Wyatt Technology) and Unicorn 5.20 (Build 500) (General Electric Company, Boston, USA).

Statistical analysis

Statistical details for each experiment can be found in the figure legends. Samples taken from cultures that were inoculated with the same pre-cultures, but propagated, nitrogen-starved and resuscitated independently in different flasks under identical conditions were considered different biological replicates. GraphPad PRISM was used to perform paired Student’s t-tests to determine the statistical significance. Asterisks in the figures were used to symbolize the p-value: One asterisk represents $p \leq 0.05$, two asterisks $p \leq 0.01$, three asterisks $p \leq 0.001$, and four asterisks $p \leq 0.0001$.

Data availability

Proteome raw data files acquired by mass spectrometry were deposited at the ProteomeXchange Consortium via the Proteomics Identifications Database partner repository[33] under the identifier PXD024024. FOR REVIEWERS ONLY: Username: reviewer_pxd024024@ebi.ac.uk; Password: YDi7Sztw

References

1. Prats, C., Graham, T. E. & Shearer, J. The dynamic life of the glycogen granule. *J. Biol. Chem.* **293**, 7089–7098 (2018).

2. Klotz, A. & Forchhammer, K. Glycogen, a major player for bacterial survival and awakening from dormancy. *Future Microbiol.* **12**, 101–104 (2017).

3. Welkie, D. G. *et al.* A Hard Day's Night: Cyanobacteria in Diel Cycles. *Trends Microbiol.* **27**, 231–242 (2019).

4. Preiss, J. Bacterial glycogen synthesis and its regulation. *Annu. Rev. Microbiol.* 419–458 (1984).

5. Forchhammer, K. & Schwarz, R. Nitrogen chlorosis in unicellular cyanobacteria – a developmental program for surviving nitrogen deprivation. *Environ. Microbiol.* **21**, 1173–1184 (2019).

6. Schwarz, R. & Forchhammer, K. Acclimation of unicellular cyanobacteria to macronutrient deficiency: Emergence of a complex network of cellular responses. *Microbiology* **151**, 2503–2514 (2005).

7. Klotz, A. *et al.* Awakening of a Dormant Cyanobacterium from Nitrogen Chlorosis Reveals a Genetically Determined Program. *Curr. Biol.* **26**, 2862–2872 (2016).

8. Doello, S., Klotz, A., Makowka, A., Gutekunst, K. & Forchhammer, K. A specific glycogen mobilization strategy enables rapid awakening of dormant cyanobacteria from chlorosis. *Plant Physiol.* **177**, 594–603 (2018).

9. Spät, P., Klotz, A., Rexroth, S., Maček, B. & Forchhammer, K. Chlorosis as a developmental program in cyanobacteria: The proteomic fundament for survival and awakening. *Mol. Cell. Proteomics* **17**, 1650–1669 (2018).

10. Liu, L., Hu, H. H., Gao, H. & Xu, X. D. Role of two phosphohexomutase genes in glycogen synthesis in Synechocystis sp. PCC6803. *Chinese Sci. Bull.* **58**, 4616–4621 (2013).

11. Osanai, T. *et al.* Pathway-level acceleration of glycogen catabolism by a response regulator in the cyanobacterium synechocystis species PCC 6803. *Plant Physiol.* **164**, 1831–1841 (2014).

12. Gründel, M., Scheunemann, R., Lockau, W. & Zilliges, Y. Impaired glycogen synthesis

causes metabolic overflow reactions and affects stress responses in the cyanobacterium Synechocystis sp. PCC 6803. *Microbiol. (United Kingdom)* **158**, 3032–3043 (2012).

13. Mihara, S. *et al.* Thioredoxin regulates G6PDH activity by changing redox states of OpcA in the nitrogen-fixing cyanobacterium Anabaena sp. PCC 7120. *Biochem. J.* **475**, 1091–1105 (2018).

14. Hagen, K. D. & Meeks, J. C. The Unique Cyanobacterial Protein OpcA Is an Allosteric Effector of Glucose-6-phosphate Dehydrogenase in Nostoc punctiforme ATCC 29133. *J. Biol. Chem.* **276**, 11477–11486 (2001).

15. Lee, Y., Stiers, K. M., Kain, B. N. & Beamer, L. J. Compromised catalysis and potential folding defects in in vitro studies of missense mutants associated with hereditary phosphoglucomutase 1 deficiency. *J. Biol. Chem.* **289**, 32010–32019 (2014).

16. Bian, Y. *et al.* An enzyme assisted RP-RPLC approach for in-depth analysis of human liver phosphoproteome. *J. Proteomics* **96**, 253–262 (2014).

17. Gururaj, A., Barnes, C. J., Vadlamudi, R. K. & Kumar, R. Regulation of phosphoglucomutase 1 phosphorylation and activity by a signaling kinase. *Oncogene* **23**, 8118–8127 (2004).

18. Bro, C., Knudsen, S., Regenberg, B., Olsson, L. & Nielsen, J. Improvement of galactose uptake in Saccharomyces cerevisiae through overexpression of phosphoglucomutase: Example of transcript analysis as a tool in inverse metabolic engineering. *Appl. Environ. Microbiol.* **71**, 6465–6472 (2005).

19. Jin, G. Z. *et al.* Phosphoglucomutase 1 inhibits hepatocellular carcinoma progression by regulating glucose trafficking. *PLoS Biol.* **16**, 1–27 (2018).

20. Malinova, I. *et al.* Reduction of the cytosolic phosphoglucomutase in Arabidopsis reveals impact on plant growth, seed and root development, and carbohydrate partitioning. *PLoS One* **9**, 1–11 (2014).

21. Seibold, G. M. & Eikmanns, B. J. Inactivation of the phosphoglucomutase gene pgm in Corynebacterium glutamicum affects cell shape and glycogen metabolism. *Biosci. Rep.* **33**, 645–654 (2013).

22. Müller, S. *et al.* Crystal structure analysis of the exocytosis-sensitive phosphoprotein, pp63/parafusin (phosphoglucomutase), from paramecium reveals significant conformational variability. *J. Mol. Biol.* **315**, 141–153 (2002).

749 23. Beamer, L. J. Mutations in hereditary phosphoglucomutase 1 deficiency map to key
750 regions of enzyme structure and function. *J. Inherit. Metab. Dis.* **38**, 243–256 (2015).

751 24. Koch, M., Doello, S., Gutekunst, K. & Forchhammer, K. PHB is produced from
752 Glycogen turn-over during nitrogen starvation in Synechocystis sp. PCC 6803. *Int. J.*
753 *Mol. Sci.* **20**, 1942 (2019).

754 25. Doello, S., Burkhardt, M. & Forchhammer, K. The essential role of sodium
755 bioenergetics and ATP homeostasis in the developmental transitions of a
756 cyanobacterium. *Curr. Biol.* **31**, 1–10 (2021).

757 26. Hauf, W. *et al.* Metabolic changes in Synechocystis PCC6803 upon nitrogen-
758 starvation: Excess NADPH sustains polyhydroxybutyrate accumulation. *Metabolites* **3**,
759 101–118 (2013).

760 27. Makowka, A. *et al.* Glycolytic shunts replenish the Calvin-Benson-Bassham cycle as
761 anaplerotic reactions in Cyanobacteria. *Mol. Plant* **13**, 471–482 (2020).

762 28. Sweetlove, L. J. & Fernie, A. R. The role of dynamic enzyme assemblies and substrate
763 channelling in metabolic regulation. *Nat. Commun.* **9**, 2136 (2018).

764 29. Rippka, R., Deruelles, J., Waterbury, J. B., Herdman, M. & Stanier, R. Y. Generic
765 Assignments, Strain Histories and Properties of Pure Cultures of Cyanobacteria.
766 *Microbiology* **111**, 1–61 (1979).

767 30. Schlebusch, M. & Forchhammer, K. Requirement of the nitrogen starvation-induced
768 protein s110783 for polyhydroxybutyrate accumulation in synechocystis sp. strain PCC
769 6803. *Appl. Environ. Microbiol.* **76**, 6101–6107 (2010).

770 31. Osanai, T. *et al.* Genetic engineering of group 2 σ factor SigE widely activates
771 expressions of sugar catabolic genes in Synechocystis species PCC 6803. *J. Biol.*
772 *Chem.* **286**, 30962–30971 (2011).

773 32. Rappsilber, J., Mann, M. & Ishihama, Y. Protocol for micro-purification, enrichment,
774 pre-fractionation and storage of peptides for proteomics using StageTips. *Nat. Protoc.*
775 **2**, 1896–1906 (2007).

776 33. Perez-Riverol, Y. *et al.* The PRIDE database and related tools and resources in 2019:
777 Improving support for quantification data. *Nucleic Acids Res.* **47**, D442–D450 (2019).

778